Title:

Uterine slow wave: directionality and changes with imminent delivery

Authors, affiliations:

Monica Albaladejo-Belmonte, Centro de Investigación e Innovación en Bioingeniería, Universitat Politècnica de València, Edif. 8B, Camino de Vera SN, 46022 Valencia, Spain

Gema Prats-Boluda, Centro de Investigación e Innovación en Bioingeniería, Universitat Politècnica de València, Edif. 8B, Camino de Vera SN, 46022 Valencia, Spain

Yiyao Ye-Lin, Centro de Investigación e Innovación en Bioingeniería, Universitat Politècnica de València, Edif. 8B, Camino de Vera SN, 46022 Valencia, Spain

Robert E Garfield, U College of Medicine, University of Arizona, 1501 N Campbell Ave, Tucson, AZ 85724, USA,

Javier Garcia-Casado, Centro de Investigación e Innovación en Bioingeniería, Universitat Politècnica de València, Edif. 8B, Camino de Vera SN, 46022 Valencia, Spain

Correspondence:

Javier Garcia-Casado, jgarciac@ci2b.upv.es

Funding:

This study was funded by Generalitat Valenciana in Programa para la promoción de I+D+i ACIF/2021/012, AICO/2021/126; the Spanish Ministry of Economy and Competitiveness, the European Regional Development Fund (MCIU/AEI/FEDER, UE RTI2018-094449-A-I00-AR).

ABSTRACT

Objective. The slow wave (SW) of the electrohysterogram (EHG) may contain relevant information on the electrophysiological condition of the uterus throughout pregnancy and labor. Our aim was to assess differences in the SW as regards the imminence of labor and the directionality of uterine myoelectrical activity.

Approach. The SW of the EHG was extracted from the signals of the Icelandic 16-electrode EHG database in the bandwidth [5, 30] mHz and its power, spectral content, complexity and synchronization between the horizontal (X) and vertical (Y) directions were characterized by the root mean square (RMS), dominant frequency (domF), sample entropy (SampEn) and maximum cross-correlation (CCmax) of the signals, respectively. Significant differences between parameters at time-to-delivery (TTD) ≤7 vs. >7 days and between the horizontal vs. vertical directions were assessed.

Main results. The SW power significantly increased in both directions as labor approached (TTD≤7d vs. >7d (mean±SD): RMS_x= 0.12±0.10 vs. 0.08±0.06mV; RMS_y= 0.12±0.09 vs. 0.08±0.05mV), as well as the dominant frequency in the horizontal direction ($domF_x$= 9.1±1.3 vs. 8.5±1.2mHz) and the synchronization between both directions (CC_{max}= 0.44±0.16 vs. 0.36±0.14). Furthermore, its complexity decreased in the vertical direction ($SampEn_y$= $6.13\cdot10^{-2}\pm8.7\cdot10^{-3}$ vs. $6.50\cdot10^{-2}\pm8.3\cdot10^{-3}$), suggesting a higher cell-to-cell electrical coupling. Whereas there were no differences between the SW features in both directions in the general population, statistically significant differences were obtained between them in individuals in many cases.

Significance. Our results suggest that the SW of the EHG is related to bioelectrical events in the uterus and could provide objective information to clinicians in challenging obstetric scenarios.

Keywords*:* electrohysterogram, slow wave, delivery, labor, directionality

INTRODUCTION

The electrohysterogram (EHG) is the surface electromyogram signal from the uterus recorded on the abdomen generated by changes in the myometrial smooth muscle cells' transmembrane potential, which propagates through the conductive tissues (Laforet et al., 2011). Two waveforms are usually identified in the EHG: a slow wave (SW), with a bandwidth that ranges from approximately 5 to 30 mHz and whose existence has been associated with slow variations of the uterine transmembrane potential (Garfield et al., 2021). The other is a fast wave (FW) with a bandwidth that goes from around 0.1 Hz to 3 Hz, divided into FW low and FW high, which have been associated with the propagation of uterine activity and uterine excitability, respectively (Devedeux et al., 1993).

The FW of the EHG has been widely studied in the literature and the analysis of its characteristics has provided new insights into electrophysiological processes and changes in the pregnant uterus throughout gestation and labor. Several authors have described an increase in FW amplitude as pregnancy advances, accompanied by a shift of its spectral content towards higher frequencies and reduced complexity (Almeida et al., 2022; Devedeux et al., 1993; Mas-Cabo et al., 2020a). However, the literature is more controversial as regards the directionality of its propagation, while some authors have described a preferentially downward propagation, others have reported upward and multidirectional propagation as well as a simultaneous upward and downward propagation (Rabotti and Mischi, 2015). Regarding the clinical utility of the FW, its features have been exploited to develop and implement predictive systems of labor (Alberola-Rubio et al., 2017; Vlemminx et al., 2018) (especially preterm labor (9,10)), and the possible success of labor induction (Benalcazar-Parra et al., 2019).

On the other hand, few studies have been devoted to assessing the SW. The first that reported the SW in the EHG was by Dill and Maiden (Dill and Maiden, 1946), who performed recordings from both the abdominal and uterine surfaces of pregnant women during labor. A decade later Larks et al (Larks et al., 1957; Larks and Dasgupta, 1958) described the amplitude, duration and shape of SW activity from the abdominal surface. They described it as a regular slow negative deflection preceded by a diphasic complex of the recorded potential with a mean amplitude of 6.74 mV, a duration of several minutes and a period equal to that of the uterine contraction, whose presence was associated with the electrical recovery/repolarization of the uterine muscle. Hon and Davis (Hon and Davis, 1958) later recorded the SW from both the abdominal surface and the peritoneal surface of the uterine fundus in early labor. The first signal, less constant and predictable, consisted of a slow potential drift of 4-5 mV over intervals of 20-25 minutes and another slow potential drift of 1-2 mV over shorter intervals. The second signal consisted of monophasic negative deflections of about 0.5 mV that occurred at the same time as changes in the intrauterine pressure signal.

The SW then ceased to be the focus of research and, unlike the FW, advances in signal processing techniques were not exploited to study the uterine myoelectrical behavior by analyzing the characteristics of this EHG component. The main reason is that its bandwidth overlaps with that of the artifacts generated by the fluctuation of the skin-electrode potential and motion artifacts due to cable movements, changes in skin stretching or electrode movements, so that its physiological origin is questioned (Devedeux et al., 1993). In a recent study, Garfield et al assessed SW directionality before labor and in its different stages by EHG recordings obtained in three directions (left-right, up-down and front-back) (Garfield et al., 2021). Particularly, they assessed the relationship between the amplitudes of the SW in the X, Y and Z directions, and described a predominantly downward directionality of the SW with the progression of labor. However, their analysis did not study other aspects, like the spectral, non-linear or coupling characteristics of this signal component. Several studies on the FW have proved that these features are strongly influenced by electrophysiological changes in the uterus during gestation and labor (Garcia-Casado et al., 2018; Huber et al., 2019), so that their study could provide additional relevant information on the electrical behavior of the uterus.

The aim of the present study was thus to characterize the SW of the pregnant uterus and to assess how it changes according to the directionality of the activity (horizontal, vertical) and the imminence of labor.

MATERIALS AND METHODS

Database composition

The study was carried out on the Icelandic 16-electrode EHG database, composed of 122 EHG recordings of 45 pregnant women (Alexandersson et al., 2015) at different gestational ages.

The sessions lasted from 8 to 86 minutes and 16 monopolar EHG signals were recorded using a four-by-four square grid of disposable Ag/AgCl electrodes placed on the patient's abdomen halfway between the uterine fundus and pubic symphysis, as well as two additional electrodes (reference and ground) positioned on the hips (see (Alexandersson et al., 2015)). The distance between electrode centers was 17.5 mm. Signals were low-pass filtered over 100Hz, digitalized to 16 bits and sampled at 200Hz.

EHG preprocessing

Following the method used in the most recent study on the SW as a reference (Garfield et al., 2021), the myoelectrical activity was characterized in the vertical and horizontal directions of the largest possible uterine area. Two raw bipolar signals ($rEHG_a(t)$, $rEHG_b(t)$) were obtained from the raw monopolar EHG signals recorded by the corner electrodes of the four-by-four grid (Cardoso, 2018; Sousa, 2015), numbered as 1, 4, 13, 16(Alexandersson et al., 2015). The inter-electrode distance for these signals is 41% greater than it would be for 'direct' vertical and bipolar signals.

$$rEHG_a(t) = rEHG_{13}(t) - rEHG_4(t) \qquad (1)$$

$$rEHG_b(t) = rEHG_1(t) - rEHG_{16}(t) \qquad (2)$$

Their projections on the X and Y axis of the Cartesian coordinates system ($rEHG_x(t)$, $rEHG_y(t)$) were calculated and summed (45º clockwise rotation) to specifically study the characteristics of the uterine myoelectrical activity in the horizontal and vertical directions (see Figure 1):

$$rEHG_x(t) = rEHG_a(t) \cdot \cos\ (45º) + rEHG_b(t) \cdot \cos\ (135º) \qquad (3)$$

$$rEHG_y(t) = rEHG_a(t) \cdot \sin\ (45º) + rEHG_b(t) \cdot \sin\ (135º) \qquad (4)$$

The SW of both signals ($SW_x(t)$, $SW_y(t)$) was extracted by applying a band-pass Butterworth filter (4th-order, zero-lag) in the bandwidth [5, 30] mHz to the corresponding raw bipolar signals ($rEHG_x(t), rEHG_y(t)$) (Devedeux et al., 1993). They were then down-sampled to 4 Hz and the three first and last minutes of the recording were discarded to prevent the stabilization time of the skin-electrode interphase and the digital filters, as well as the artifacts associated with manipulating the equipment or the patient's movements at the end of the recording, from influencing the analysis.

Recordings of less than 30 minutes with prominent artifacts and/or that had been acquired from women who had delivered prematurely, i.e. with a gestational age lower than 37 weeks, were not analyzed. These patients were not included in the analysis, given the lack of information on the influence of this obstetric scenario on the SW characteristics. The recording sessions were grouped according to the imminence of delivery (TTD ≤ 7d: 27 recordings; TTD>7d: 83 recordings) (Lemancewicz et al., 2016; Mas-Cabo et al., 2019).

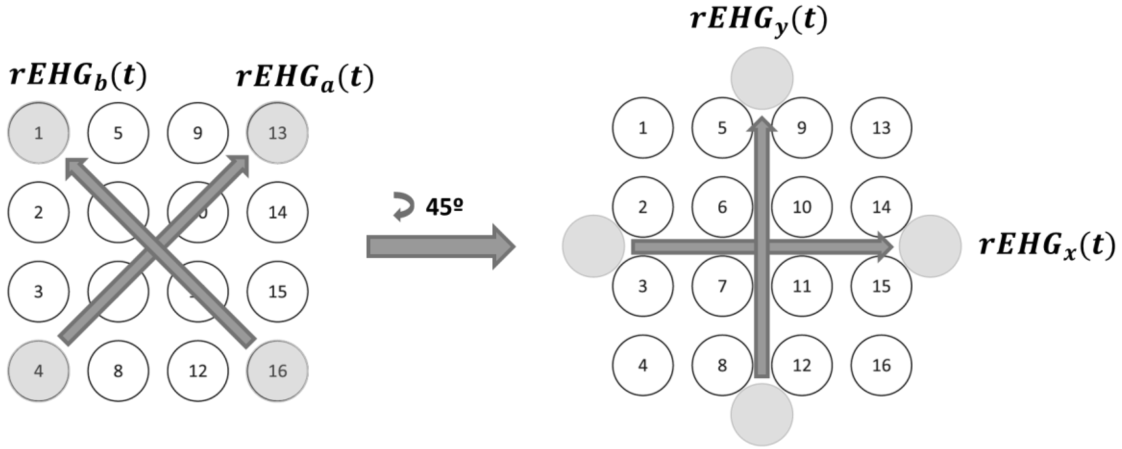

Figure 1. Scheme of the EHG bipolar signals aligned with the horizontal and vertical directions ($rEHG_y$ and $rEHG_x$, right) from original bipolar recordings ($rEHG_a$ and $rEHG_b$, left).

SW parametrization

The FW of the EHG ([0.2-4] Hz) is typically studied in sliding windows of 120s (Mas-Cabo et al., 2020b; Prats-Boluda et al., 2021). As the period of the SW ranges from 33.3s to 200s, a larger analysis window was required, therefore a window length of 500s was selected. As the aim of the present study was to get a detailed insight into the uterine SW activity rather than implementing or testing novel signal metrics, four parameters that assess different signal characteristics and whose use and interpretation have been broadly addressed in the literature were computed from sliding windows (80% overlap) of $SW_x(t)$ and $SW_y(t)$: root mean square (*RMS*), dominant frequency (*domF*), sample entropy (*SampEn*) and maximum cross correlation (CC_{max}).

Root Mean Square (RMS)

Given a discrete time series $x[n]$ of *N* samples, its *RMS* is computed as follows:

$$RMS = \sqrt{\frac{\sum_{i=1}^{N} x[i]^2}{N}} \quad (5)$$

In surface electromyography, and particularly in electrohysterography, the *RMS* of the signal is a robust measure of its amplitude and power, the reason why it was computed in the present study to characterize SW activity. Higher *RMS* values are associated with increased rates of temporal and spatial recruitment of muscle fibers (Farina et al., 2004).

Dominant frequency (domF)

The *domF* of a signal is the frequency at which its power spectral density (PSD) is maximal (Phinyomark et al., 2012). In this study, the signal PSD was estimated with autoregressive models (1000th order). The dominant frequency has been typically used to assess the repetition frequency of the SW of other biosignals such as those from the stomach or the small bowel (Garcia-Casado et al., 2005; Ye-Lin et al., 2009), the reason why it was selected in the present study to assess SW spectral content.

Sample Entropy (SampEn)

SampEn is a non-linear measure defined as the negative natural logarithm of the conditional probability that two segments within a given numerical series of length *N* that are similar at m samples ($m < N$) are still similar at m+1 samples, according to a tolerance *r* and ignoring self-matches (Richman et al., 2004). Like other entropy metrics, *SampEn* measures the complexity or randomness of the signal's information, so that greater values are associated with an increased rate of information production (Delgado-Bonal and Marshak, 2019). *SampEn* was chosen to characterize SW complexity since it has been used in previous studies on the EHG FW (di Marco et al., 2014; Garcia-Gonzalez et al., 2013; Mischi et al., 2018) more than other non-linear indices such as approximate entropy, fuzzy entropy or spectral entropy.

Maximum cross correlation (CCmax)

The cross correlation (*CC*) of two numerical series $a[n]$ and $b[n]$ measures the linear correlation between them when one of them is lagged τ samples with respect to the other:

$$\boldsymbol{CC(\tau)} = \frac{\boldsymbol{E}\left[(\boldsymbol{a}[\boldsymbol{n}]-\overline{\boldsymbol{a}})\left(\boldsymbol{b}[\boldsymbol{n}+\boldsymbol{\tau}]-\overline{\boldsymbol{b}}\right)^{*}\right]}{\boldsymbol{\sigma}(\boldsymbol{a}[\boldsymbol{n}])\cdot\boldsymbol{\sigma}(\boldsymbol{b}[\boldsymbol{n}])} \qquad (6)$$

Where E, $\overline{}$, * and σ are the expected value, mean, conjugate transpose and standard deviation operators, respectively. *CCmax* is the maximum absolute value of CC for all possible τ delays and it ranges from 0 to 1. In surface electromyography, and thus in electrohysterography, values near to 1 are associated with high across-muscle synchronization, while values close to 0 are associated with low across-muscle synchronization (Keenan et al., 2007). *CCmax* was used to characterize SW activity since it is a simple and fast-to-compute index to assess coupling between two time series (Stacey et al., 2020).

RMS, *domF* and *SampEn* were computed for each window of $SW_x(t)$ and $SW_y(t)$ separately, while *CCmax* was calculated for each pair of time-matching windows of $SW_x(t)$ and $SW_y(t)$.

Data analysis

The SW features of each recording session were summarized from two approaches (*Approach I*, *Approach II*) and, for each of these two statistical studies were carried out to assess any differences between the characteristics of the SW in both directions (*Study A*) and of both TTD groups (*Study B*).

In *Approach I* the median value of the parameter in windows of $SW_x(t)$ and of $SW_y(t)$ was computed. In this approach, *Study A* consisted of comparing the distributions of the medians of the SW feature in $SW_x(t)$ vs. $SW_y(t)$, separately for each TTD group (TTD≤7d, TTD>7d), according to a paired sample T-test or a Wilcoxon signed-rank test -depending on the normality of data- at the 5% significance level. *Study B* compared the distributions of the medians of the SW features in TTD ≤ 7d vs. TTD > 7d, separately for each direction (X, Y), according to a two sample T-test or a Mann-Whitney U test -depending on the normality of data- at the 5% significance level

Approach II was implemented to specifically consider the degree of dissimilarities between the SW of both directions of the individual recordings, regardless of the existence of any fixed trend of differences in the total population. In this approach the difference of the parameter value in each pair of time-matching windows of $SW_x(t)$ and $SW_y(t)$ in the recording sessions was computed and the distribution of this difference was statistically compared to 0 (according to a paired sample T-test or a Wilcoxon signed-rank test, depending on the normality of data at the 5% significance level). The recording session was thus included in the X>Y, Y>X or X=Y group, depending on whether the distribution of the difference of the parameter was statistically greater than 0 (X>Y), lower than 0 (Y>X) or not different from 0 (X=Y). In this approach, *Study A* consisted of assessing whether there was an equal proportion (33%) of X=Y, X>Y and Y>X recordings within a given TTD group according to the Chi-square goodness of fit test at the 5% significance level. In *Study B,* significant differences between the percentage of recordings of each group (X=Y, X>Y and Y>X) in TTD ≤ 7d vs. TTD > 7d were assessed according to the Chi-square test of independence at the 5% significance level. Post hoc analysis considering Bonferroni correction were conducted in both studies.

Table 1 shows an overview on the statistical analyses and summarization approaches performed on each SW feature.

Table 1. Summary on the approaches used to synthesize the information of each recording (Approach I, Approach II) and the statistical studies (Study A-directionality, Study B-labor imminence) performed to assess the differences in the root mean square (*RMS*), dominant frequency (*domF*), sample entropy (*SampEn*) and maximum cross correlation (*CCmax*) of the slow wave (SW) characteristics, depending on the directionality of the activity and labor imminence. [TTD: time to delivery. d: days]

		RMS	**domF**	**SampEn**	**CCmax**
Approach I Differences directly assessed at population level	**Study A** Comparison of medians of: SW_x vs. SW_y (TTD≤7d) SW_x vs. SW_y (TTD>7d)	x	x	x	
	Study B Comparison of medians of: TTD≤7d vs. TTD>7d (SW_x) TTD≤7d vs. TTD>7d (SW_y)	x	x	x	x
Approach II Differences assessed firstly at patient level and secondly at population level	**Study A** Comparison of proportions: [X=Y] = [X>Y] = [Y>X] (TTD≤7d) [X=Y] = [X>Y] = [Y>X] (TTD>7d)	x	x	x	
	Study B Comparison of proportions: TTD≤7d vs. TTD>7d (X=Y) TTD≤7d vs. TTD>7d (X>Y) TTD≤7d vs. TTD>7d (Y>X)	x	x	x	

RESULTS

Figure 2 shows 1000s of the SW obtained from EHGs recorded in the horizontal (top panels) and vertical (bottom panels) directions in two women with TTDs ≤7 days (left) and >7 days (right), respectively. It can be seen that the signal reached higher peak-to-peak amplitudes in the first than the second patient in both directions.

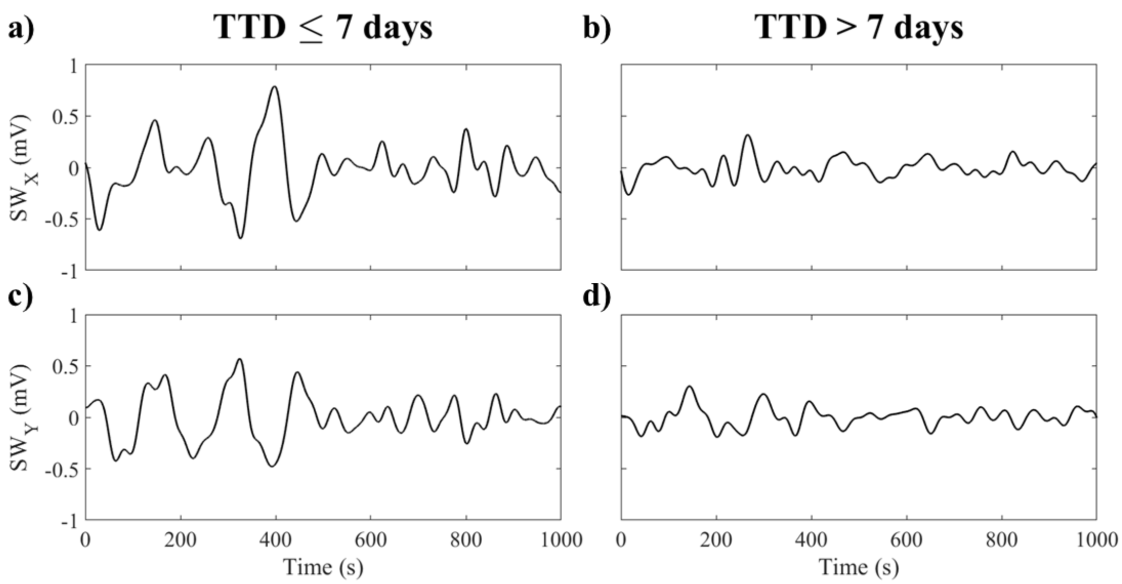

Figure 2. Slow waves of the electrohysterogram in the horizontal ($\boldsymbol{SW_X}$, panels (a) and (b)) and vertical ($\boldsymbol{SW_Y}$, panels (c) and (d)) direction from two patients with TTDs less than or equal to 7 days (TTD ≤ 7 days, panels (a) and (c)) and higher than 7 days (TTD > 7 days, panels (b) and (d)).

Figure 3 shows the box-whisker plot of the median values of each parameter of the recording sessions (Approach I) considering each direction (X, Y) separately and delivery group (TTD≤7 days, >7 days). Significantly different pairs of distributions (p-value < 0.05) in Study A and B are marked with asterisks.

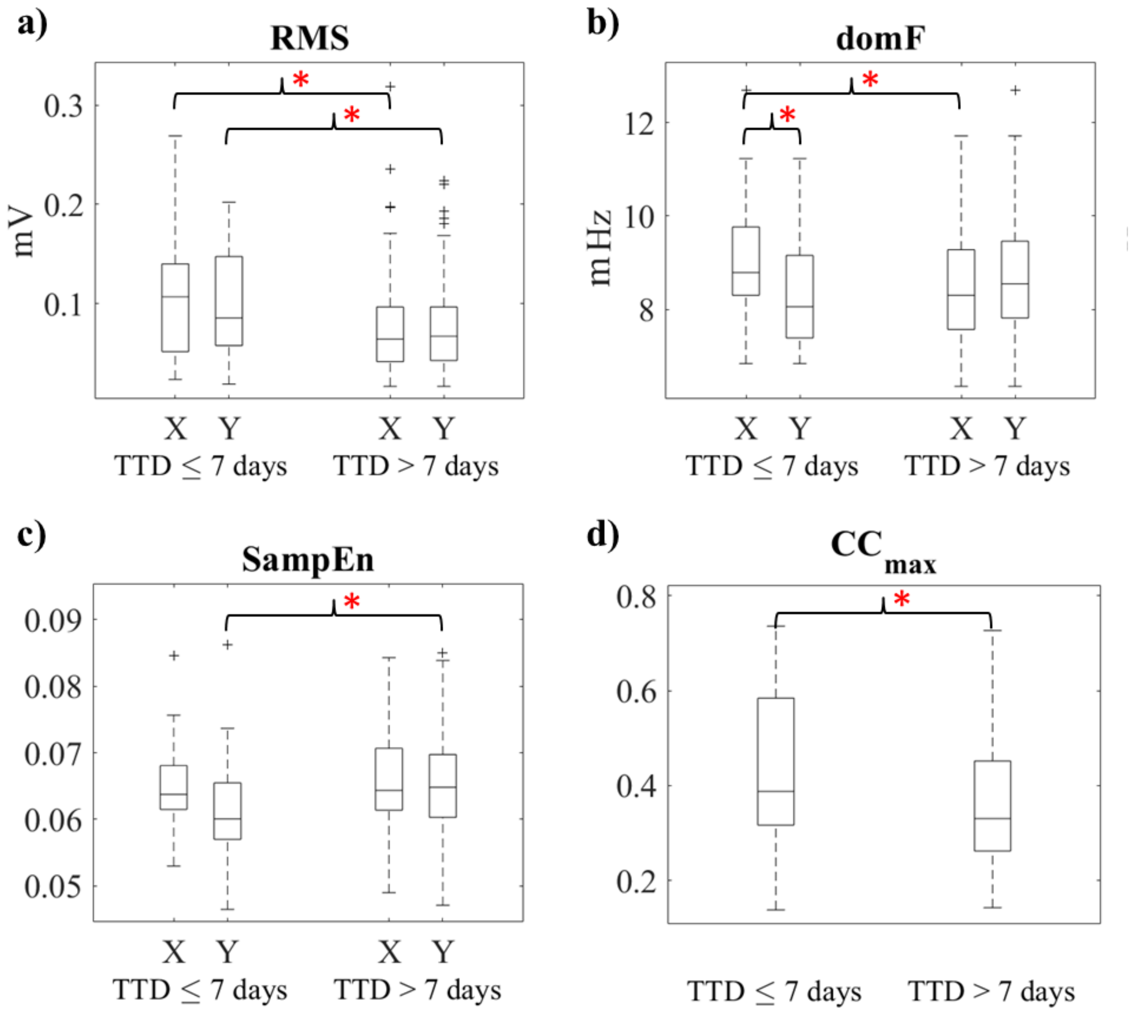

Figure 3. Box-whisker plots of the a) root mean square (RMS), b) dominant frequency (domF), c) sample entropy (SampEn) of the slow waves of the horizontal (X) and vertical (Y) directions and d) maximum cross correlation (CCmax) between them in patients with TTDs less than or equal to 7 days (≤7 days) and higher than 7 days (>7 days). Red asterisk: statistically significant difference (confidence level: 5%) between the distributions shown under the ends of the brace.

In Study A there were no statistically significant differences between the characteristics of the SW recorded in each direction with both TTD ≤7 days or > 7days. The only exception was the *domF* of the SW in TTD≤7 days group, whose value was significantly greater in the X direction than in the Y ($domF_X = 9.1 \pm 1.3$ mHz vs. $domF_Y = 8.3 \pm 1.2$ mHz). In the comparisons between the TTD groups (Study B), the *RMS* of the SW was significantly greater in TTD≤7 days than in TTD>7 days in both directions ($RMS_X =$

0.12 ± 0.10 mV vs. 0.08 ± 0.06 mV; $RMS_Y = 0.12 \pm 0.09$ mV vs. 0.08 ± 0.05 mV, respectively). Conversely, there were significant differences between the *domF* and *SampEn* of the SW of both TTD groups only in one of the two directions: the *domF* was significantly greater in TTD≤7 days than the other only in the X direction ($domF_x = 9.1 \pm 1.3$ mHz vs. 8.5 ± 1.2 mHz, respectively), while *SampEn* was significantly lower only in the Y direction ($SampEn_y = 6.1 \cdot 10^{-2} \pm 0.9 \cdot 10^{-2}$ vs. $6.5 \cdot 10^{-2} \pm 0.8 \cdot 10^{-2}$, respectively). For CC_{max}, median values were lower than 0.5 in both TTD groups and were significantly higher in TTD ≤7 days than TTD >7 days ($CC_{max} = 0.44 \pm 0.16$ vs. 0.36 ± 0.14 , respectively).

Figure 4 gives the results obtained when the data from each recording session were summarized in Approach II, showing the percentage of recordings belonging to the TTD groups with *RMS*, *domF* and *SampEn* values not significantly different between the windows of both SW signals (X=Y), significantly greater in their SW_x windows than in those of their SW_y (X>Y) and vice versa (Y>X). Percentages of X=Y, X>Y and Y>X recordings significantly different than 33% for each TTD group (Study A) are highlighted with an asterisk. In the *RMS* and *SampEn* parameters, for which Approach I showed no significant differences in directionality in the total population, the X=Y group could be expected to be significantly predominant in individual patients, although the X<Y and X>Y groups accounted for more than 50% of the recordings for both TTD groups. In domF, the X=Y group percentage was significantly higher than the rest for both TTD groups. In Study B, the percentage of cases of both X<Y and X>Y groups was always smaller (greater similarity between directions in individual patients) for TTD≤7days than >7days (except for X>Y in SampEn), although no statistically significant differences were found in any case between both TTD groups.

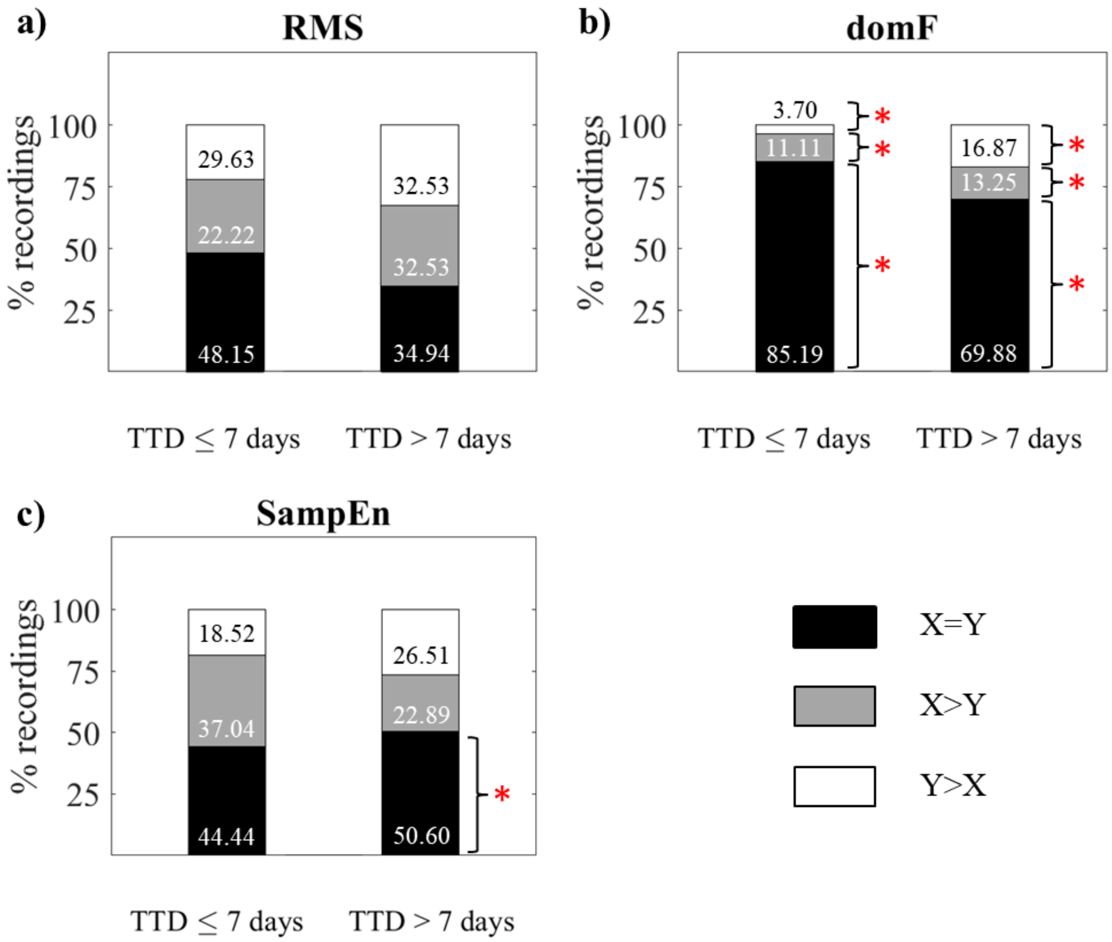

Figure 4. Percentage of recordings in which the a) root mean square (*RMS*), b) dominant frequency (*domF*), c) sample entropy (*SampEn*) of the slow waves were equal in both directions (X=Y), significantly greater in the horizontal than in vertical direction (X>Y) and vice versa (Y>X) in patients with TTDs lower than or equal to 7 days (TTD≤7 days) and higher than 7 days (TTD>7 days). Red asterisk: proportion significantly different from the expected value (confidence level: 5%).

DISCUSSION

The present study assessed differences in the characteristics of uterine SW activity by their directionality analyzed by the Cartesian projections (horizontal, vertical) and the imminence of labor in the Icelandic 16-electrode EHG database (Alexandersson et al., 2015).

In *Approach I*, the results showed that there were no differences between the SW characteristics in both directions, indicating that no direction (X or Y) of the SW Cartesian decomposition prevailed over the other in the total population, regardless of the imminence of labor. The only exception was the dominant frequency, which was greater in the horizontal than vertical direction in the imminent delivery group (TTD≤7d). This finding suggests that electrophysiological events originating SW activity show a higher repetition frequency when labor is closer.

On the other hand, there were several significant differences between the SW parameters between women far and close to delivery (Study B), particularly with higher power, (assessed by *RMS*) and dominant frequency and lower complexity of information (assessed by *SampEn*) in imminent deliveries, in agreement with the electrophysiological changes found in the FW (Devedeux et al., 1993; Mas-Cabo et al., 2020a). As delivery approaches uterine excitability increases (Wray and Arrowsmith, 2021), so that the rise in SW power could be associated with a greater number of activated excitable myometrial cells and their discharge rate (Farina et al., 2004). Furthermore, the higher conduction velocity of electrical signals across the uterus as pregnancy progresses (Smith et al., 2015) and the transition of excitable cells from independent oscillators to a highly coupled system able to generate organized contractions (Banney et al., 2015) would justify the changes observed in the SW spectral content and regularity, respectively. It should also be pointed out that when both TTD groups were compared, significant differences were found in SW power in both directions, but in SW spectral content and complexity only in one of the two directions (horizontal in the first and vertical in the second). This suggests that the electrophysiological changes experienced by the uterus as parturition approaches affect the bioelectrical activity differently in both directions (Anderson et al., 1981) .

The synchronization between horizontal and vertical SW activity directions was also assessed by quantifying the degree of resemblance of both waveforms' morphology (assessed by their *CCmax*). In agreement with previous studies on the FW (Mas-Cabo et al., 2018), our results showed higher synchronization when parturition was close than longer than a week after the recording session. This finding agrees with other studies in the literature that found that cell-to-cell coupling increases during pregnancy and especially in labor thanks to a rise in the number and permeability of gap junctions (Nadir Çiray et al., 1994; Sakai et al., 1992). On the other hand, the present study analyzed bipolar signals obtained from the corner electrodes of the four-by-four grid, so that they provided information on the myoelectrical activity of a relatively large uterine area. Coupling within the myometrium at this global level mainly occurs during labor, when the fetus is about to be expelled (Garfield and Maner, 2007), while we considered a wide TTD threshold (7 days) for imminent delivery. A stricter threshold (0-1 day) would probably have yielded greater CC values for this group, since the most remarkable electrophysiological changes take place one or two days before delivery, or at most seven days before in premature births (Maner et al., 2003).

The aim of the second approach used to summarize the myoelectrical information of the recording sessions was to consider specific differences between the SW in both directions in individual recordings, since we considered that the parameter's median value throughout the whole recording session would only be able to provide vague information on this aspect. The differences between horizontal and vertical EHG features were thus assessed in individual patients before comparing the different groups. According to our results, the power and complexity of the SW in both directions was at most equal in half of the recordings for both TTD groups, while in the remainder they were greater in the horizontal than vertical direction in a similar number of cases. This indicates differences between the characteristics of the activity in both directions in a significant number of cases, but balanced in terms of 'predominant' directionality. This could explain why no significant differences were found in the total population (Approach I). On the other hand, the dominant frequency in both directions was similar in most recordings, regardless of the imminence of labor, which could have been influenced by the narrow bandwidth of the SW ([5, 30] mHz) and the frequency resolution of its PSD (2 mHz). We also found a trend towards greater similarity between both directions in individuals when labor was imminent, although these were not statistically significant.

The latest study on the SW was performed by Garfield *et al.* (2021), who obtained and analyzed the vector electromyometriogram of SWs recorded in the X and Y directions of pregnant women at term not in labor and also in its first and second stages. They reported that the loop of the vector did not show any predominant direction in women who were not in labor, while it pointed mainly downward in those who were in labor, which can be interpreted as a larger vertical than horizontal SW amplitude. As indicated above, in the present study SW amplitude was not significantly greater in either direction with TTDs longer than a week, which agrees Garfield's results, although we found this to be so when labor was near. The main reason could be that the close-to-parturition group included signals from women suspected to be in labor with others who delivered up to seven days after the recording, so that we did not specifically assess changes in the SW throughout labor, as did Garfield and colleagues. They also analyzed activity in the [30, 100] mHz

EHG bandwidth rather than in the [5, 30] mHz bandwidth, which means that remnant FW activity could still be present in their SW signal, given the closeness of both bandwidths (Devedeux et al., 1993). Finally, interelectrode distances were considerably greater in their work than in ours, which means they could detect the SW activity of a wider area.

As described in the Methods section, to characterize global uterine SW activity in horizontal and vertical directions we obtained bipolar signals from the furthest electrodes in the grid and performed a 45º rotation. To test the reliability of the preprocessing, we also analyzed the bipolar signals recorded by each pair of electrodes on the edges of the four-by-four grid and aligned with the X and Y axes. We obtained the same SW difference trend with respect to labor imminence -greatest power and dominant frequency and lower complexity of information- but with less statistical significance (results not shown).

The present study was limited by the impossibility of directly relating the analyzed bioelectrical signal to electrophysiological events. The origin of the SW has been broadly discussed in the literature and some authors have associated it with motion artifacts caused by skin stretching (Devedeux et al., 1993; Hon and Davis, 1958). However, we believe that the EHG component between 5 and 30 mHz characterized in this study was of uterine origin for different reasons. First, if the analyzed SW was mainly generated by changes in the skin-electrode contact and/or cable movements it should only be present during intervals of contractile activity and not during basal activity, as we noticed when we visually inspected the preprocessed recordings. Secondly, no other physiological component (possible embedded interference) has been reported in the [5, 30] mHz bandwidth of the EHG, apart from the uterine SW, not even fetal and maternal electrocardiograms, whose spectral components are associated with frequencies higher than 50 mHz (Marchon and Naik, 2015). Thirdly, the electrophysiological changes found in the SW with imminent labor, which were in line with those reported in the literature on the FW, should not occur if the SW was merely a baseline fluctuation. We also investigated the possibility of the SW extracted being a remnant of the FW activity obtained after filtering the EHG, even though SW activity could be identified even in periods with no FW activity.

Another of the study's limitations was the small number of recordings in the database performed at most 24 hours before parturition, which prevented us from specifically examining the changes in SW activity in such close deliveries. As mentioned above, the use of a lax criterion to define the nearest labor group could be the reason why no differences were found between the SW in both directions, as could have been expected on the basis of the study by Garfield *et al.* (2021).

However, in spite of its limitations the study has confirmed that SW activity contains relevant information on the proximity of labor, and so could represent an indicator, not previously addressed in the literature, that could potentially help to detect imminent labor. As set forth by Devedeux *et al.* (1993), the most relevant bandwidths identified in the EHG, i.e. FW low and FW high, are associated with different aspects of the uterine myoelectrical activity such as its propagation or cells excitability. In the case of SW, its existence could be related to electrophysiological characteristics that may experience more pronounced changes with labor imminence than those related to FW, thus implying a potential advantage of using SW compared to FW to detect labor. The fact that the SW usually showed amplitude values higher than those of the FW can also be regarded as an inherent advantage of SW analysis with respect to assessing the FW, since this indicates more robustness against artifacts and noise. Furthermore, FW analysis requires the existence of contractile events in the signal, which may not appear in short recordings during pregnancy check-ups, and typically their individual annotation, which can be a cumbersome and time-consuming task. SW activity is present in contractile and noncontractile periods and its analysis does not require the identification of specific signal segments.

In future work it would be interesting to increase the sample size -particularly the number of recordings acquired on the day of parturition- and repeat the present analysis to assess variations in labor-associated SW activity in greater depth. SW characterization could be broadened with additional parameters, such as other novel non-linear metrics (e.g. phase entropy or multiscale entropy) that have shown their potential to monitor pregnancy progression (Reyes-Lagos et al., 2020), or other approaches focused on interdependences between signals of different regions (e.g. Granger causality or direct transfer entropy) that have already yielded promising results in FW analysis (Zhang et al., 2022). Further efforts should also be made to analyze any possible relationship between SW and FW temporal dynamics and whether their information is redundant or complementary in predicting term and/or preterm labor.

CONCLUSIONS

Our results show that the uterine SW experiences significant changes as delivery approaches: its power and frequency increases, the complexity of its information decreases and synchronization between the activity of the horizontal and vertical directions rises. These variations could be associated with a larger number of activated excitable uterine cells and a higher conduction velocity, accompanied by a transition of this cells from independent oscillators to a highly coupled system mediated by gap junctions.

As regards the directionality of the activity, there are no significant differences in the general population, although the SW characteristics are not always homogeneous across the horizontal and vertical directions in individual patients.

This study shows that the SW of the EHG provides relevant information on the bioelectrical behavior of the pregnant uterus. Its analysis can yield new insights into the electrophysiological processes and changes as pregnancy progresses and labor approaches. It could also develop new biomarkers for term/preterm birth or labor induction success prediction.

REFERENCES

Alberola-Rubio, J., Garcia-Casado, J., Prats-Boluda, G., Ye-Lin, Y., Desantes, D., Valero, J., Perales, A., 2017. Prediction of labor onset type: Spontaneous vs induced; role of electrohysterography? Computer Methods and Programs in Biomedicine 144, 127–133.

Alexandersson, A., Steingrimsdottir, T., Terrien, J., Marque, C., Karlsson, B., 2015. The Icelandic 16-electrode electrohysterogram database. Scientific Data 2, 1–9.

Almeida, M., Mouriño, H., Batista, A.G., Russo, S., Esgalhado, F., Palma dos Reis, C.R., Serrano, F., Ortigueira, M., 2022. Electrohysterography extracted features dependency on anthropometric and pregnancy factors. Biomedical Signal Processing and Control 75, 103556.

Anderson, G.F., Kawarabayashi, T., Marshall, J.M., 1981. Effect of indomethacin and aspirin on uterine activity in pregnant rats: comparison of circular and longitudinal muscle. Biol Reprod 24, 359–372.

Banney, D., Young, R., Paul, J.W., Imtiaz, M., Smith, R., 2015. A Hypothesis for Self-Organization and Symmetry Reduction in the Synchronization of Organ-Level Contractions in the Human Uterus during Labor. Symmetry 2015, Vol. 7, Pages 1981-1988 7, 1981–1988.

Benalcazar-Parra, C., Ye-Lin, Y., Garcia-Casado, J., Monfort-Ortiz, R., Alberola-Rubio, J., Perales, A., Prats-Boluda, G., Martínez-Villaseñor, L., 2019. Prediction of Labor Induction Success from the Uterine Electrohysterogram. Journal of Sensors 2019.

Cardoso, F.E. de O.G., 2018. Uterine Contractions Clustering Based on Surface Electromyography: An Input for Pregnancy Monitoring.

Delgado-Bonal, A., Marshak, A., 2019. Approximate Entropy and Sample Entropy: A Comprehensive Tutorial. Entropy 2019, Vol. 21, Page 541 21, 541.

Devedeux, D., Marque, C., Mansour, S., Germain, G., Duchêne, J., 1993. Uterine electromyography: A critical review. American Journal of Obstetrics and Gynecology 169, 1636–1653.

di Marco, L.Y., di Maria, C., Tong, W.C., Taggart, M.J., Robson, S.C., Langley, P., 2014. Recurring patterns in stationary intervals of abdominal uterine electromyograms during gestation. Medical and Biological Engineering and Computing 52, 707–716.

Dill, L. v., Maiden, R.M., 1946. The electrical potentials of the human uterus in labor. American Journal of Obstetrics & Gynecology 52, 735–745.

Farina, D., Merletti, R., Enoka, R.M., 2004. The extraction of neural strategies from the surface EMG. J Appl Physiol 96, 1486–1495.

Garcia-Casado, J., Martinez-De-Juan, J.L., Ponce, J.L., 2005. Noninvasive measurement and analysis of intestinal myoelectrical activity using surface electrodes. IEEE Trans Biomed Eng 52, 983–991.

Garcia-Casado, J., Ye-Lin, Y., Prats-Boluda, G., Mas-Cabo, J., Alberola-Rubio, J., Perales, A., 2018. Electrohysterography in the diagnosis of preterm birth: a review. Physiological Measurement 39, 02TR01.

Garcia-Gonzalez, M.T., Charleston-Villalobos, S., Vargas-Garcia, C., Gonzalez-Camarena, R., Aljama-Corrales, T., 2013. Characterization of EHG contractions at term labor by nonlinear analysis. Proceedings of the Annual International Conference of the IEEE Engineering in Medicine and Biology Society, EMBS 7432–7435.

Garfield, R.E., Maner, W.L., 2007. Physiology and electrical activity of uterine contractions. Seminars in Cell & Developmental Biology 18, 289–295.

Garfield, R.E., Murphy, L., Gray, K., Towe, B., 2021. Review and Study of Uterine Bioelectrical Waveforms and Vector Analysis to Identify Electrical and Mechanosensitive Transduction Control Mechanisms During Labor in Pregnant Patients. Reprod Sci 28, 838–856.

Hon, E.H.G., Davis, C.D., 1958. Cutaneous and Uterine Electrical Potentials in Labor—an Experiment. Obstetrics & Gynecology 12, 47–53.

Huber, C., Shazly, S.A., Ruano, R., 2019. Potential use of electrohysterography in obstetrics: a review article. The Journal of Maternal-Fetal & Neonatal Medicine 34, 1666–1672.

Keenan, K.G., Farina, D., Meyer, F.G., Merletti, R., Enoka, R.M., 2007. Sensitivity of the cross-correlaton between simulated surface EMGs for two muscles to detect motor unit synchronization. Journal of Applied Physiology 102, 1193–1201.

Laforet, J., Rabotti, C., Terrien, J., Mischi, M., Marque, C., 2011. Toward a multiscale model of the uterine electrical activity. IEEE Transactions on Biomedical Engineering 58, 3487–3490.

Larks, S.D., Assali, N.S., Morton, D.G., Selle, W.A., 1957. Electrical Activity of the Human Uterus in Labor. Journal of Applied Physiology 10, 479–483.

Larks, S.D., Dasgupta, K., 1958. Wave forms of the electrohysterogram in pregnancy and labor. American Journal of Obstetrics and Gynecology 75, 1069–1078.

Lemancewicz, A., Borowska, M., Kuć, P., Jasińska, E., Laudański, P., Laudański, T., Oczeretko, E., 2016. Early diagnosis of threatened premature labor by electrohysterographic recordings-The use of digital signal processing. Biocybernetics and Biomedical Engineering 36, 302–307.

Maner, W.L., Garfield, R.E., Maul, H., Olson, G., Saade, G., 2003. Predicting term and preterm delivery with transabdominal uterine electromyography. Obstet Gynecol 101, 1254–1260.

Marchon, N., Naik, G., 2015. Electrode positioning for monitoring Fetal ECG: A Review. In: Chopde, A.M., Vatti, R. (Eds.), IEEE International Conference on Information Processing. Pune, India, pp. 5–10.

Mas-Cabo, J., Prats-Boluda, G., Perales, A., Garcia-Casado, J., Alberola-Rubio, J., Ye-Lin, Y., 2019. Uterine electromyography for discrimination of labor imminence in women with threatened preterm labor under tocolytic treatment. Med Biol Eng Comput 57, 401–411.

Mas-Cabo, J., Ye-Lin, Y., Garcia-Casado, J., Alberola-Rubio, J., Perales, A., Prats-Boluda, G., 2018. Uterine contractile efficiency indexes for labor prediction: A bivariate approach from multichannel electrohysterographic records. Biomedical Signal Processing and Control 46, 238–248.

Mas-Cabo, J., Ye-Lin, Y., Garcia-Casado, J., Díaz-Martinez, A., Perales-Marin, A., Monfort-Ortiz, R., Roca-Prats, A., López-Corral, Á., Prats-Boluda, G., 2020a. Robust Characterization of the Uterine Myoelectrical Activity in Different Obstetric Scenarios. Entropy 22, 743.

Mas-Cabo, J., Ye-Lin, Y., Garcia-Casado, J., Díaz-Martinez, A., Perales-Marin, A., Monfort-Ortiz, R., Roca-Prats, A., López-Corral, Á., Prats-Boluda, G., 2020b. Robust Characterization of the Uterine Myoelectrical Activity in Different Obstetric Scenarios. Entropy 2020, Vol. 22, Page 743 22, 743.

Mischi, M., Chen, C., Ignatenko, T., de Lau, H., Ding, B., Guid Oei, S.G., Rabotti, C., 2018. Dedicated Entropy Measures for Early Assessment of Pregnancy Progression from Single-Channel Electrohysterography. IEEE Transactions on Biomedical Engineering 65, 875–884.

Nadir Çiray, H., Persson, B. -E, Bäckstrom, T., Roomans, G.M., Ulmsten, U., 1994. Direct intracellular injections for studying human myometrial gap junctions prior to labor. Acta Obstetricia et Gynecologica Scandinavica 73, 97–102.

P., S.A., Subramaniam, K., Iqbal, N. v., 2019. A review of significant researches on prediction of preterm birth using uterine electromyogram signal. Future Generation Computer Systems 98, 135–143.

Phinyomark, A., Thongpanja, S., Hu, H., Phukpattaranont, P., Limsakul, C., 2012. The Usefulness of Mean and Median Frequencies in Electromyography Analysis. In: Naik, G.R. (Ed.), Computational Intelligence in Electromyography Analysis - A Perspective on Current Applications and Future Challenges. IntechOpen, London, pp. 195–220.

Prats-Boluda, G., Pastor-Tronch, J., Garcia-Casado, J., Monfort-Ortíz, R., Perales Marín, A., Diago, V., Roca Prats, A., Ye-Lin, Y., 2021. Optimization of Imminent Labor Prediction Systems in Women with Threatened Preterm Labor Based on Electrohysterography. Sensors 2021, Vol. 21, Page 2496 21, 2496.

Rabotti, C., Mischi, M., 2015. Propagation of electrical activity in uterine muscle during pregnancy: a review. Acta Physiologica 213, 406–416.

Reyes-Lagos, J.J., Pliego-Carrillo, A.C., Ledesma-Ramirez, C.I., Peña-Castillo, M.A., Garcia-González, M.T., Pacheco-Lopez, G., Echeverria, J.C., 2020. Phase entropy analysis of electrohysterographic data at the third trimester of human pregnancy and active parturition. Entropy 22, 798.

Richman, J.S., Lake, D.E., Moorman, J.R., 2004. Sample Entropy. METHODS IN ENZYMOLOGY 384, 172–184.

Sakai, N., Tabb, T., Garfield, R.E., 1992. Modulation of cell-to-cell coupling between myometrial cells of the human uterus during pregnancy. Am J Obstet Gynecol 167, 472–480.

Smith, R., Imtiaz, M., Banney, D., Paul, J.W., Young, R.C., 2015. Why the heart is like an orchestra and the uterus is like a soccer crowd. Am J Obstet Gynecol 213, 181–185.

Sousa, C.M.M.F.C. de, 2015. Electrohysterogram signal component cataloging with spectral and time-frequency methods.

Stacey, W., Kramer, M., Gunnarsdottir, K., Gonzalez-Martinez, J., Zaghloul, K., Inati, S., Sarma, S., Stiso, J., Khambhati, A.N., Bassett, D.S., others, 2020. Emerging roles of network analysis for epilepsy. Epilepsy Res 159, 106255.

Vlemminx, M.W.C., Rabotti, C., van der Hout-Van Der Jagt, M.B., Oei, S.G., 2018. Clinical Use of Electrohysterography during Term Labor: A Systematic Review on Diagnostic Value, Advantages, and Limitations. Obstetrical and Gynecological Survey 73, 303–324.

Wray, S., Arrowsmith, S., 2021. Uterine Excitability and Ion Channels and Their Changes with Gestation and Hormonal Environment. Annu Rev Physiol 83, 331–357.

Xu, J., Chen, Z., Lou, H., Shen, G., Pumir, A., 2022. Review on EHG signal analysis and its application in preterm diagnosis. Biomedical Signal Processing and Control 71, 1746–8094.

Ye-Lin, Y., Garcia-Casado, J., Prats-Boluda, G., Ponce, J.L., Martinez-De-Juan, J.L., 2009. Enhancement of the non-invasive electroenterogram to identify intestinal pacemaker activity. Physiol Meas 30, 885–902.

Zhang, Y ;, Hao, D ;, Yang, L ;, Zhou, X ;, Ye-Lin, Y ;, Yang, Y, Zhang, Yajun, Hao, Dongmei, Yang, Lin, Zhou, Xiya, Ye-Lin, Yiyao, Yang, Yimin, 2022. Assessment of Features between Multichannel Electrohysterogram for Differentiation of Labors. Sensors 22, 3352.